Electronic Supplementary Material (ESI) for Nanoscale.

Supporting Information

Highly Versatile Platform Based on Geometrically Well-Defined 3D DNA Nanostructures for Selective Recognition and Positioning of Multiplex Targets

Ziwen Dai,[a] Qi Gao,[b] Man Ching Cheung,[a] Leung Hoi Man,[a] Terrence Chi Kong Lau,[c] Hanadi F. Sleiman,[d] King Wai Chiu Lai[b*] and Pik Kwan Lo[a*]

[a]Department of Biology and Chemistry, [b]Department of Mechanical and Biomedical Engineering, [c]Department of Biomedical Sciences, City University of Hong Kong, Tat Chee Avenue, Kowloon, Hong Kong SAR, China.[d] Department of Chemistry, McGill University, 801 Sherbrooke Street West, Montreal, QC H3A 2K6, Canada.

Materials and reagents. Acetic acid, urea, boric acid, ethylenediaminetetraacetic acid disodium salt dihydrate (EDTA), formamide, magnesium chloride hexahydrate, StainsAll®, tris(hydroxymethyl)aminomethane (Tris), *N,N,N',N'*-tetramethylethylenediamine, ammonium persulfate and glycerol were used as purchased from Sigma Aldrich. Vectabond™ reagent was purchased from Vector Laboratories. 40% acrylamide/bis-acrylamide solution (19:1) was purchased from Bio-Rad. 1000Å nucleoside-derivatized LCAA-CPG solid support with loading densities of 25-40 µmol/g, Reagents used for automated DNA synthesis were purchased from BioAutomation. Sephadex G-25 (super fine DNA grade) was used as purchased from Amersham Biosciences. 1 X TAMg buffer was composed of 45 mM Tris, 7.6 mM $MgCl_2$, with pH adjusted to 8 using glacial acid. 1 X TBE buffer was composed of 90 mM Tris and boric acid, 1.1 mM EDTA, with a pH of ~ 8. Microscopic glass coverslips (12mm) were purchased from Bragg & Co. Grade SPI-1 Highly ordered pyrolytic graphite (HOPG) was purchased from SPI. Fluorescein-labeled insulin was purchased from NANOCS. Alexa Fluor 647-labeled ATP was purchased from Thermo Fisher Scientific, and thrombin from human plasma was purchased from Sigma Aldrich.

Instrumentation. Gel scanning was performed on a Fujifilm FLA-9000 scanner. Fluorescence measurements were conducted on HORIBA Jobin Yvon™ FluoroMax-4 spectrofluorometer. Standard automated oligonucleotide solid-phase synthesis was performed on BioAutomation MerMade MM6 DNA synthesizer. UV-Vis measurements were carried out on Shimadzu™ UV-1700 PharmaSpec UV-Vis spectrophotometer. Gel electrophoresis experiments were carried out on an acrylamide 20 X 20 cm Maxi Vertical electrophoresis apparatus (MV-20DSYS). Confocal fluorescence imaging was performed on Laser Confocal Scanning Microscope (Leica TCS SP5) with magnification of 63X. Fluorescence anisotropy measurement was performed on HORIBA FluoroLog Spectrophotometer FL3-22. Agarose gel electrophoresis was performed on Bio-Rad Mini-Sub Cell GT Cell Apparatus with a 7 X 7 cm gel tray.

DNA sequences

	Sequence (5’→3’)	ε_{260} [L/(mole • cm)]
TL	TATTGGTTTGVTGACCAATAACACAAATCGGVTCAGTAATCTCTTGAAGGTAVGGAAACGACA	710200
T	TATTGGTTTGTGACCAATAACACAAATCGGTCAGTAATCTCTTGAAGGTAGGAAACGACA	710200
CS1	TCGGCAGACTCTACTTGGTGCAAACCAATATGTCGTTTCCGGCGGCGTTAAATAGACGCGGCCA	608300
CS2	CGGTGCATTTAGTCGTGTCGCCGATTTGTGTTATTGGTCACGCGAATCATGCGTACTCGT	559300
CS3	CCATAGCTTTCTCAGCAGCGAAAATACCTTCAAGAGATTACTGAGTCTTGGAGTCGGATTGAGC	621800
LS1-Thr	TGAGAAAGCTATGGCACGTCTGGAAGGATTGGTTGGTGTGGTTGGTTTCCTTCCTCCCGATGGCCGCGTCTATT	689600
LS2-ATP	AAATGCACCGGCTACCAGGTGCGCGTTACCTGGGGGAGTATTGCGGAGGAAGGTGTCACATTACGCGCTTGAATTTCAAGCTCAATCCG	854600
LS3-Ins	AGTCTGCCGAGCTACCAGGTTTGGTGGTGGGGGGGGTTGGTAGGGTGTCTTCTTGAATTTCAAACGAGTACGC	699300
LS1	TGAGAAAGCTATGGCACGTCACCGATGGCCGCGTCTATT	371800
LS2	AAATGCACCGGCTACCAGGTGAATTTCAAGCTCAATCCG	376700
LS3	AGTCTGCCGAGCTACCAGGTGAATTTCAAACGAGTACGC	380200
Tt	CAAACCAATATGTCGTTTCC	189800
RS1	TAACGCCGCCTTTTTTCGCTGC	185700
RS2	ACTCCAAGACTTCGACACGACT	209600
RS3-Cy5	(Cy5)ATGATTCGCGTTCACCAAGTAG	216200
RS3	ATGATTCGCGTTCACCAAGTAG	216200

RS3-biotin	(Biotin)ACTCCAAGACTTCGACACGACT	209600
dsLS23	TTGAAATTCACCTGGTAGC	181700
dsLS23-Cy3	TTGAAATTCATT(Cy3)TTCCTGGTAGC	215100
dsLS1	TCGGTGACGTG	104600
dsLS1-Cy3	TCGGTGTT(Cy3)TTACGTG	138400

- a human α-thrombin binding aptamer (a 15-mer oligonucleotide with a sequence of 5'-GGTTGGTGTGGTTGG-3'),
- an ATP binding aptamer (a 33-mer oligonucleotide with a sequence of 5'-ACCTGGGGGAGTATTGCGGAGGAAGGTGTCACA-3')
- an insulin binding aptamer (a 30-mer oligonucleotide with a sequence of 5'-GGTGGTGGGGGGGGTTGGTAGGGTGTCTTC-3')

Self-assembly of DNA nanotubes

Initial efforts focused on the preparation of triangular-shaped DNA rung (R) from a closed DNA template (T). By mixing T with equivalent amount of three complementary DNA strands (CS1, CS2 and CS3) and three short DNA strands (RS1, RS2 and RS3) sequentially, R was formed quantitatively with short sticky-end overhangs (Scheme S1).

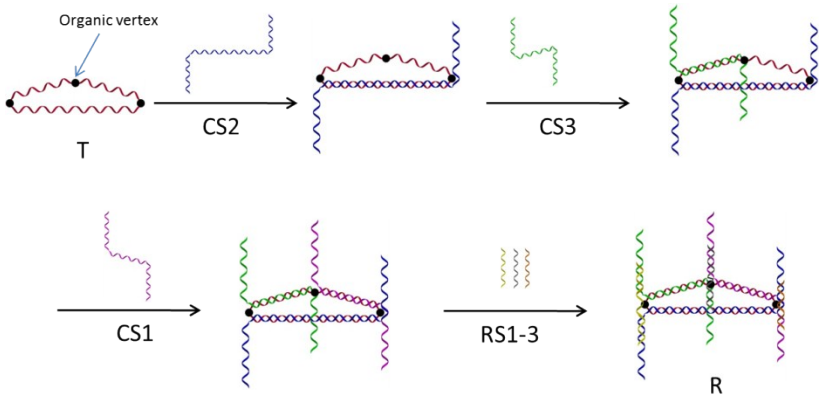

Scheme S1 Schematic representation showing the formation of the triangular-shaped DNA rung (R) from a closed DNA template (T).

The self-assembly of DNA nanotubes was carried out according to the previously reported methods by Sleiman and coworkers.[i] Typically, 77.4 pmoles of the purified T and equimolar amounts of strands CS1, CS2, CS3, RS1, RS2, RS3 and 3 µL of 1X TAMg buffer were combined and dried completely with Eppendorf™ Concentrator *Plus* and re-dissolved in 30 µL of autoclaved water. The mixture was first heated to 95 ℃ and then slowly cooled down to 4 ℃ over about 5 h. This would generate a triangular rung **R** (Scheme S1). Then equimolar amounts of dsLS1 and LS1-Thr, dsLS23 and LS3-Ins, dsLS23 and LS2-ATP were also combined in 10 µL of 0.1X TAMg buffer and annealed from 95 ℃ to 4 ℃ over ~ 5 h to form Thr-ds-LS1, ATP-ds-LS2 and Ins-ds-LS3. Finally, two solutions were mixed and annealed from 60 ℃ to 4 ℃ over 3 h to form the desired DNA nanotubes **3Apt-DNANTs**.

Gel characterizations

All the DNA strands were checked by 15% denaturing polyacrylamide gel electrophoresis (PAGE) in 1X TBE buffer (composed of 90 mMTris and boric acid, 1.1 mM EDTA, with a pH of ~ 8). 8% Native PAGE was performed in 1X TAMg buffer (composed of 45 mM Tris, 7.6 mM $MgCl_2$, with pH adjusted to 8 using glacial acid). 0.8% or 4.5% agarose gel electrophoresis was performed in 1X TAE buffer, see Fig S3 (composed of 40 mM Tris, 20 mM acetic acid and 1 mM EDTA with a pH~8.3).

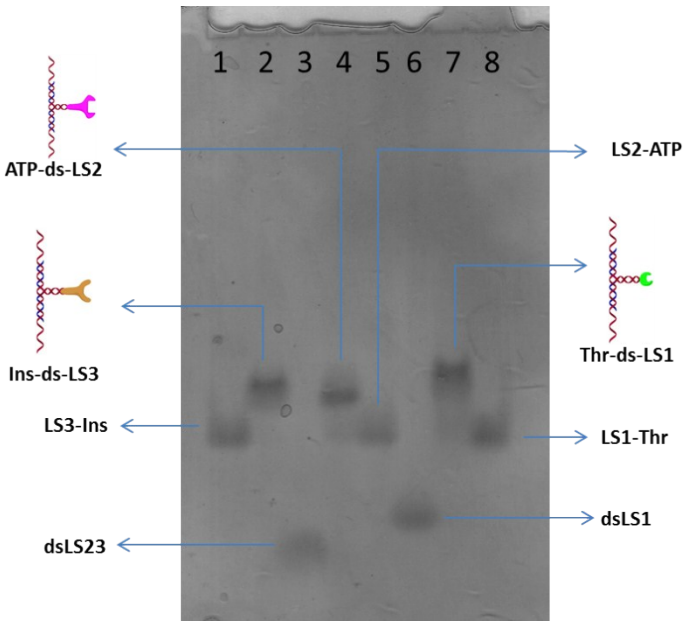

Figure S1. Native polyacrylamide gel electrophoresis (PAGE) analysis of the formation of double-stranded linking strands Thr-ds-LS1, ATP-ds-LS2 and Ins-ds-LS3.

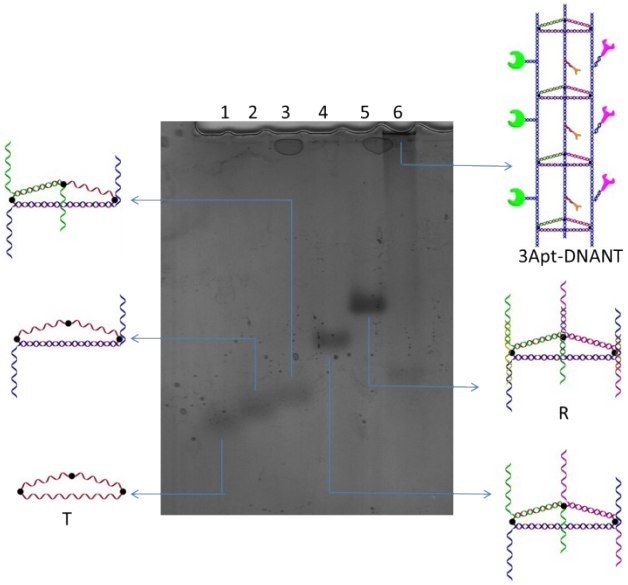

Figure S2. Native PAGE analysis of the formation of the polymeric DNA assemblies **3Apt-DNANTs**.

To clearly demonstrate the co-existing of the three aptamers onto the single nanotube, we synthesized the three binding aptamers with fluorophore labeling such as FAM-labeled thrombin binding aptamer, Texas Red-labeled ATP binding aptamer and Cy3-labeled insulin binding aptamer. Using the same assembly strategy, 3Apt-DNANTs were formed with three fluorophores on top. To eliminate the unhybridized fluorophore-labeled aptamers in solution, the nanotube samples were centrifuged using the Microcon-10kDa centrifugal filters with Ultracel-10 membrane to filter the excess or unhybridized aptamers. After the filtration, UV-vis measurements were performed accordingly (Figure S3a). We clearly observed three distinguishable absorption peaks at 498 nm, 550 nm and 596 nm which are corresponded to the FAM, Cy3 and Texas Red fluorophores respectively from the fluorophore-labeled 3Apt-DNANTs. Unlabeled 3Apt-DNANTs (control) were also prepared and then mixed with the three fluorophore-labeled aptamers in excess for UV-vis measurements. We only can observe the three absorption peaks in the filtrate, but not in the residue of the unlabeled 3Apt-DNANTs. These confirmed that the filtration is useful to get rid of the excess or unhybridized aptamers and ensure these obtained UV-vis signals (black curve) were come from the well-formed fluorophore-labeled 3Apt-DNANTs. The native PAGE analysis also confirmed the co-existing of the three aptamers onto a single nanotube by showing a very low mobility DNA band with three fluorescence signals (Figure

S3b, lane 1) while excess, three individual fluorophore-labeled aptamers were separated from unlabeled 3Apt-DNANTs after filtration process (Figure S3b, lane 3).

a.

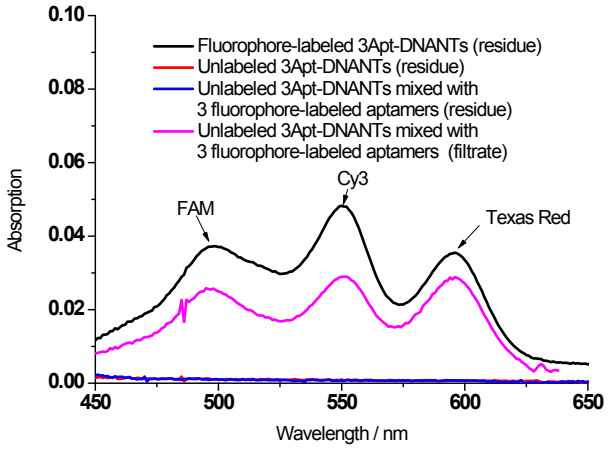

b.

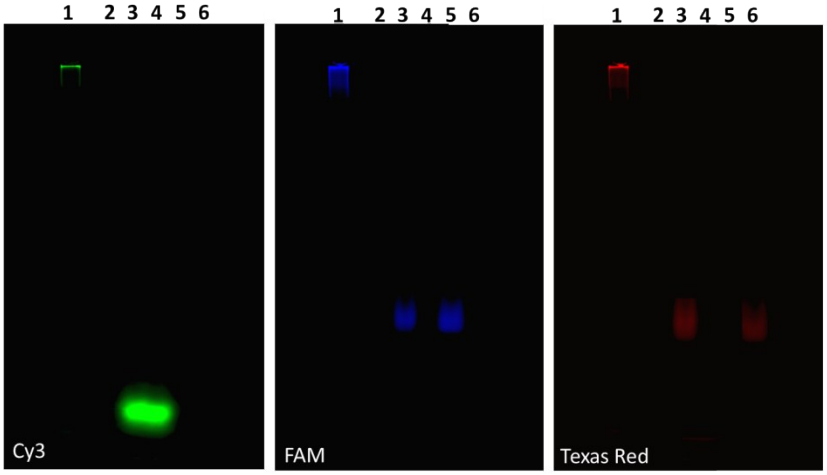

Figure S3. Native PAGE analysis of the DNA samples after filtration. Lane 1: Fluorophore-labeled 3Apt-DNANTs, lane 2: Unlabeled 3Apt-DNANTs, lane 3: Unlabeled 3Apt-DNANTs mixed with 3 fluorophore-labeled aptamers (filtrate), lane 4: Cy3-labeled insulin binding aptamer, lane 5: FAM-labeled thrombin binding aptamer, lane 6: Texas Red-labeled ATP binding aptamer.

Confocal imaging of DNA nanotubes on coverslips

The coverslips used for confocal imaging were treated following the reported protocol by Sleiman and coworkers. The 22 X 22 mm micro cover glasses from VWR™ were immersed in

Piranha solution (70%/30% concentrated sulfuric acid/ 30% H_2O_2) for at least 2 h and then rinsed with de-ionized water 3 times with sonication for 10 min each time. The coverslips were then rinsed with HPLC grade acetone 3 times with sonication for 10 min each time and then dried at 120℃ to remove any trace of water. The dried coverslips were immersed in 0.5 mL of VectaBond™ dispersed in 25 mL of HPLC grade acetone for 2 min followed by being rinsed with deionized water. After drying with N_2 flow, the coverslips were immersed in 20 mL of 0.1 M sodium bicarbonate solution containing 50 mg of biotin-mPEG-SVA (average MW=5000 g/mol) in 20 mL solution for 3 h. Then the coverslips were gently rinsed with biograde water (from 1st Base Pte Ltd) 3 times and dried with N_2 flow. 50 µL of 1 mg/mL avidin in PBS solution was dispersed in 10 ml PBS buffer and the coverslips were immersed in the avidin solution for 3 h. After that coverslips were rinsed gently with biograde water 3 times and dried under N_2 flow. The dried coverslips were placed on clean aluminum foil in a Petri dish and the biotin (on RS3 strand) anchored nanotube samples (5.2 µM in 30 µL) were dropped onto the coverslips and left with lid covered for 3 h. Then the coverslips were rinsed gently with biograde water and immersed in 6 mL of 1 mg/ml staining solution (V-carbozole) for 2 h. Then the coverslips were rinsed with biograde water 3 times and were ready for confocal imaging.

Electrophoretic Mobility Shift Assay (EMSA)

Electrophoretic Mobility Shift Assay (EMSA) was performed to explore the specific binding between the Thr-DNANTs and thrombin proteins. As shown in Figure 2a (target : DNA nanotube ratios between 0.5 : 1 and 3 : 1), with higher concentration of thrombin for Thr-DNANT system, the bands corresponding to the free DNA nanotubes were fainter, and bands corresponding to the slower migrating DNA nanotube/target complexes appeared. No broken DNA building blocks were observed. To confirm the specific molecular recognition between DNA-aptamer nanotubes and the targets, control DNA nanotubes with the sequence dT_n incorporated instead of the aptamer sequences were also characterized by EMSA (Figure S3). The DNA band intensity of free, control DNA nanotubes did not change

before and after addition of the targets. This revealed no significant binding between control DNA nanotube and thrombin.

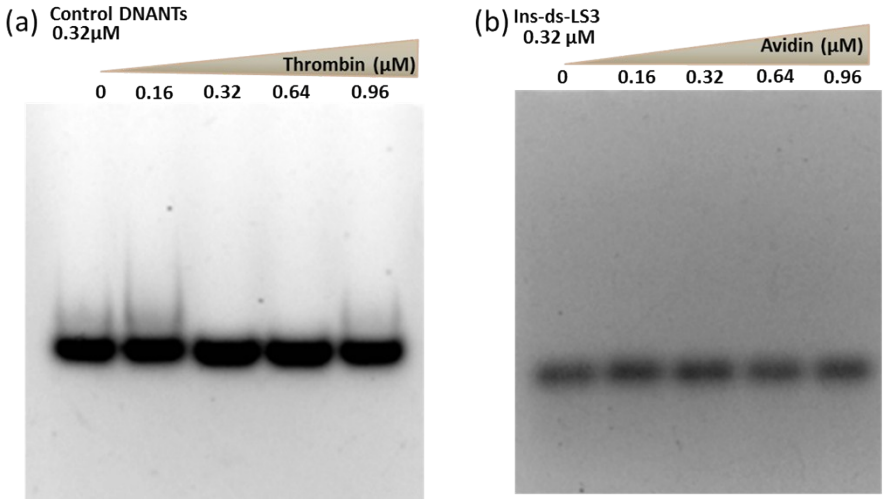

Figure S4 EMSA assay of agarose gel analysis confirming (a) no specific binding between control DNA nanotubes and thrombin proteins and (b) no specific binding between DNA building blocksIns-ds-LS3and avidin. The concentration of the sample mixture loaded in each lane is indicated above the gel.

Fluorescence resonance energy transfer and fluorescence enhancement experiments

Fluorescence resonance energy transfer experiments (FRET) and fluorescence enhancement experiments were performed on HORIBA Jobin Yvon^{TM} FluoroMax-4 spectrofluorometer. To observe the FRET signal or fluorescence enhancement, the nanotube was modified with corresponding fluorophore respectively. 3-methyl isoxanthopterin (3-MI) was replacing the 7th G in the thrombin-binding aptamer, Insulin was modified with FITC and the Insulin-binding aptamer nanotube was modified with Cy3 in the middle of strand dsLS23 (Scheme S2). ATP was labeled with Alexa 647, and ATP-binding aptamer nanotube was modified with Cy3 in the middle of strand dsLS23.Typically, the self-assembled DNA nanotubes consisting of 9.63 pmoles of T and equimolar amount of the rest strands were incubated with equal molar amount of target molecules (human α-thrombin, FITC-labeled insulin, Alexa 647 labeled ATP) for 15 min, and then diluted to 120 μL and the fluorescence emission spectra were collected. For thrombin-binding aptamer nanotube, 3-MI was excited at 350 nm, and emission was collected from 375 nm to 475 nm. For Insulin-binding aptamer

nanotube, FITC was excited at 475 nm, and emission was collected from 500 nm to 540 nm for monitoring FITC emission and 540 nm to 640 nm for monitoring Cy3 emission. For ATP-binding aptamer nanotube, Cy3 was excited at 514 nm and emission was collected from 540 nm to 630 nm for monitoring Cy3 emission and 640 nm to 750 nm for monitoring Alexa 647 emission. Control samples were prepared by incubating the modified nanotube with control protein avidin or trypsin.

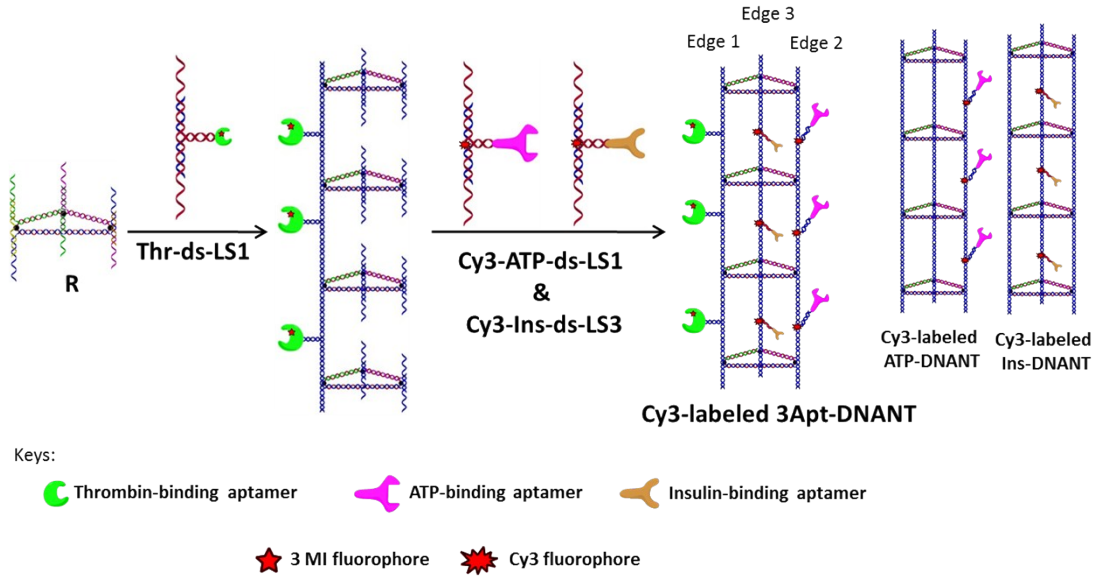

Scheme S2. Construction of Cy3-labeled 3Apt-DNANT.

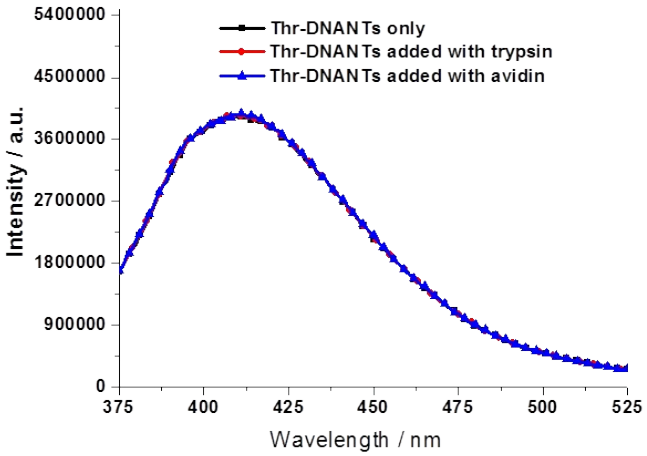

Figure S5. Fluorescence spectra for the Thr-DNANTs consisting of signaling aptamer with 80 nM of trypsin or avidin.

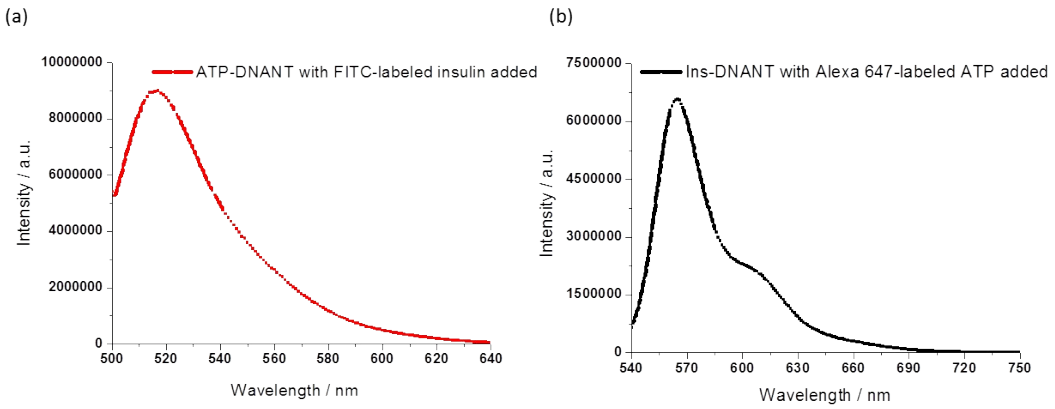

Figure S6. FRET spectra for the (a) FITC-labeled insulin/ATP-DNANTs mixture, and (b) Alexa 647-labeled ATP/ins-DNANTs mixture.

TEM Imaging

Transmission electron microscopy (TEM) was carried out on a FEI/Philips Tecnai 12 BioTWIN Transmission Electron Microscope under vacuum with an operation mode of 120 kV. Typically 15 µL (5 µL X 3 times) of the assembled nanotube solution (consisting of 9.63 pmoles of T strand and equimolar amount of the rest strands with an overall concentration of 5.2 µM) was deposited on carbon films on 200 mesh grids copper. The drying was accelerated by Eppendorf™ Concentrator Plus and the freshly dried sample was stained by being placed with the sample side covered on a drop of 10 µL of NanoVan™ solution for 1 min and dried with Kimwipe tissue followed by being placed on a drop of 10 µL of deionized water for another 1 min. Then the sample was roughly dried with Kimwipe tissue and dried in Eppendorf™ Concentrator Plus for 30 min and then moved into a desiccator prior to imaging.

TEM was used to directly visualize the DNA nanotubes before and after the addition of the thrombin (Figure S6). Two different staining agents including NanoVan (for DNA staining) and ammonium molybdate (for protein staining) were used. TEM images showed that apparent tubular images were acquired when the thrombin/Thr-DNANTs complexes were stained with ammonium molybdate (right image) but no such observation is obtained when the same sample was stained with NanoVan (left image). On the other hand, no clear tubular feature of the Thr-DNANTs was observed after being stainged with ammonium molybdate.

These TEM results further confirmed the specific molecular recognition and binding of thrombin to Thr-DNANTs.

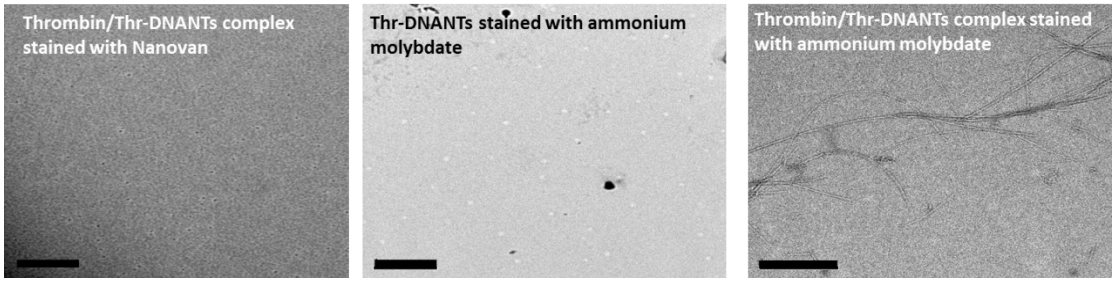

Figure S7. Negative staining of TEM images of Thr-DNANTs and thrombin/Thr-DNANT complex. Scale bar is 1μm.

Fluorescence anisotropy measurements and K_d calculation

Fluorescence anisotropy measurement was performed on HORIBA FluoroLog Spectrophotometer FL3-22 with a built-in data collection and processing software package FluorEssence 2.0 powered by Origin 7.5. Typically, self-assembled DNA nanotube consisting of 0.963 pmoles of T and equimolar amount of the rest strands were incubated with corresponding targets for 15 min before conducting anisotropy measurement. The target concentrations were prepared as 0.2, 0.4, 0.6, 0.8, 1, 1.5, 2, 2.5 times of the nanotube concentration (0.13 μM) in moles. Anisotropy was collected using emission anisotropy with a width of 40 nm from maxima of the fluorophore (e.g. 3MI, Alexa 647, FITC) emission. Each anisotropy measurement was performed twice.

To test the intrinsic performance of the aptamer-functionalized DNA nanotubes by fluorescence anisotropy-based assay, we conducted titration experiments on each type of nanotubes using a cuvette-based fluorescence spectrometer. Typical change in anisotropy data are shown in Figure S7 and Table S1 for thrombin/Thr-DNANTs, Alexa 647-labeled ATP/ATP-DNANTs and FITC-labeled insulin/Ins-DNANTs.

Since there were many binding sites along the edges of the nanotube, this calculated K_d was just an apparent dissociation constant.

If the binding between an aptamer and its target was in equilibrium,

$AB \rightleftharpoons A + B$

Then the dissociation constant could be defined as:

$K_d = \frac{[A][B]}{[AB]}$ …… (Eq. 1)

Here, A was defined as the aptamer nanotube and B was defined as the corresponding target.

Before the aptamer was added to the system, anisotropy came from the free fluorescently labeled B. When the aptamer nanotube was gradually added to the system, anisotropy came from free B and bounded B in the complex AB.

Anisotropy changes came from the binding between A and B, suppose that

$\Delta_A \propto [AB]$

$\because K_d = \frac{[A][B]}{[AB]}$ and $[A]_0=[A]+[AB]$

$\therefore K_d = \frac{([A]0 - [AB])[B]}{[AB]}$

$\therefore [AB] = \frac{[A]0[B]}{Kd + [B]}$ …… (Eq. 2)

Since $\Delta_A \propto [AB]$

Let

$\Delta_A = k*[AB]$ where k was a constant.

$\Delta_A = k * \frac{[A]0[B]}{Kd + [B]}$

$\therefore \frac{1}{\Delta A} = \frac{Kd + [B]}{k * [A]0[B]}$ …… (Eq. 3)

$= K_d * \frac{1}{k * [A]0} * \frac{1}{[B]} + \frac{1}{k * [A]0}$

Now, $\frac{1}{\Delta A}$ was plotted against $\frac{1}{[B]}$ as a linear regression

slope=$\frac{1}{k * [A]0} * Kd$ and intercept=$\frac{1}{k * [A]0}$

∴K_d=slope/intercept ……. (Eq.4)

And plot $\frac{1}{\Delta A}$ against $\frac{1}{[B]}$ and we get

a. For thrombin and Thr-DNANTs

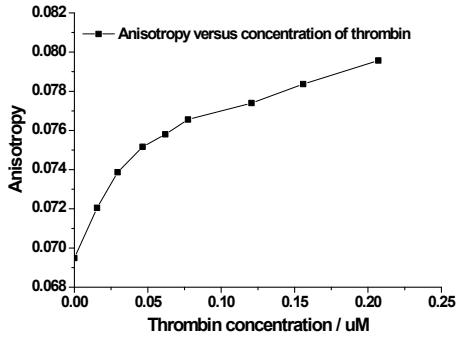

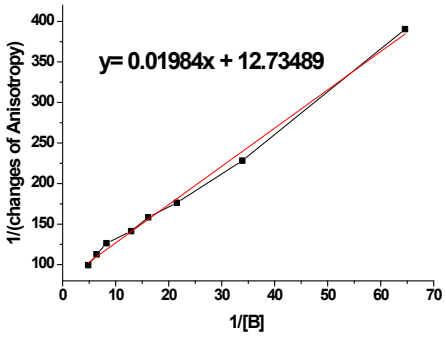

b. For Alexa 647-labeledATP and ATP-DNANTs

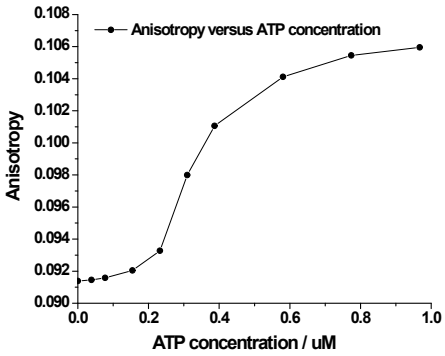

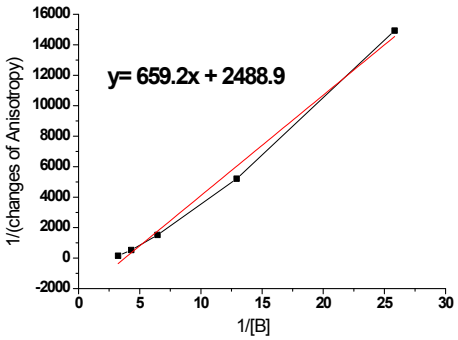

c. For FITC-labeled insulin and Ins-DNANTs

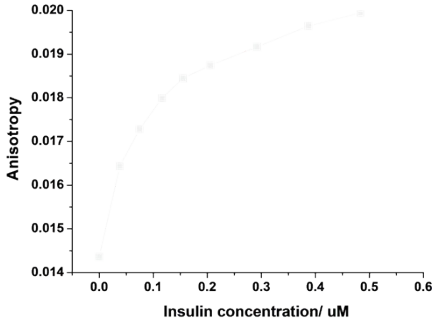

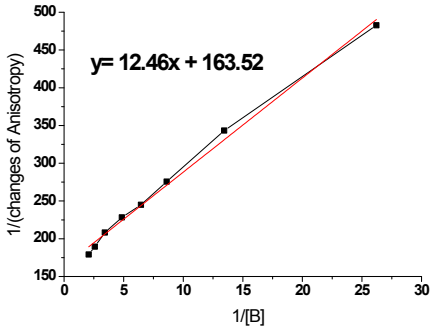

Figure S8. Fluorescence anisotropy and binding curve of (a) 64 nMThr-DNANTs, (b) 64 nMATP-DNANTs and (c) 64 nMIns-DNANTs with increasing concentrations of thrombin, ATP and insulin respectively.

	Slope	**Intercept**	**K_d (nM)**
Thrombin and Thr-DNANTs	0.01984	12.73489	1.56± 0.02
Alexa 647-labeled ATP and ATP-DNANTs	659.2	2488.9	265 ± 19
FITC-labeled Insulin and Ins-DNANTs	12.46	163.52	76.2± 6.7

Table S1 The fitted of the data with equation 4 yield the dissociation constants (K_d) for the thrombin sensing, ATP sensing and insulin sensing in the solution-phase measurements.

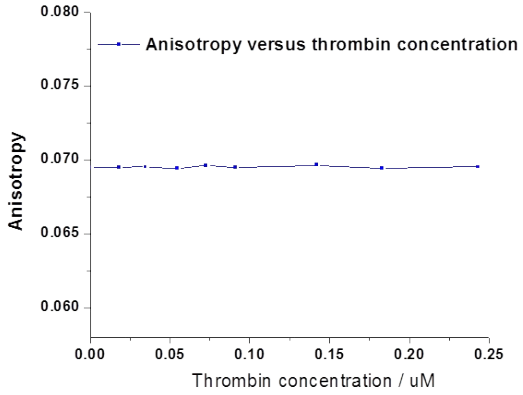

Figure S9. Fluorescence anisotropy of 160 nM regular DNA nanotubes (without the aptamer sequences) with increasing concentrations of thrombin.

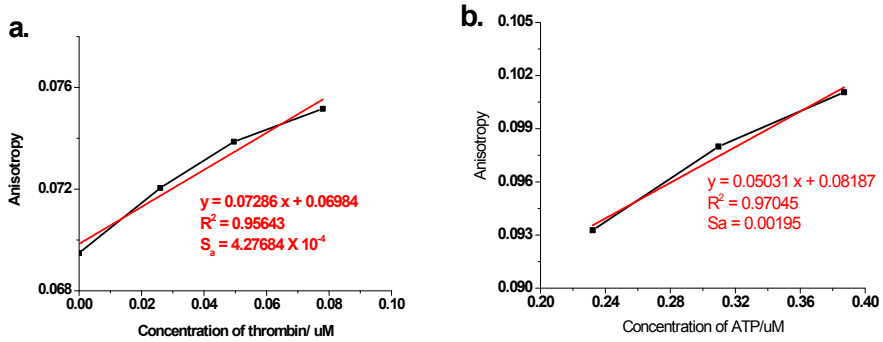

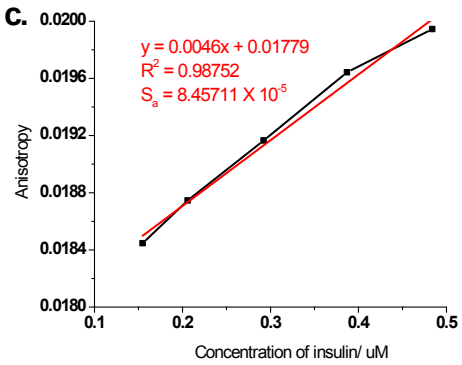

Figure S10 The linear relationship between fluorescence anisotropy and the concentrations of (a) thrombin, (b) ATP and (c) insulin.

Detection of multiplex targets

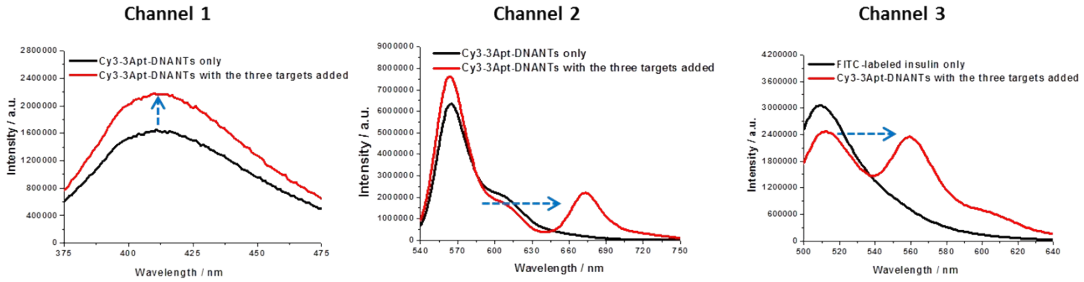

Figure S11. Simultaneous measurement of the fluorescence change of the 0.2μM Cy-3 labeled 3Apt-DNANTs before and after an addition of the three targets including 0.2 μM thrombin, 0.2 μM ATP and 0.2 μM insulin (Sample 1). Channel 1 monitors the fluorescence intensity enhancement of 3MI by exciting at 350 nm and collecting the emission signals from 375 nm to 475 nm; channel 2 monitors the FRET signal of Alexa 647 labeled-ATP by exciting the Cy3 fluorophore at 514 nm and collecting the emission signals from 640 to 750 nm; channel 3 monitors the FRET signal of Cy3 fluorophore-labeled nanotubes by exciting the FITC fluorophore at 475 nm and collecting the emission signals from 550 to 640 nm.

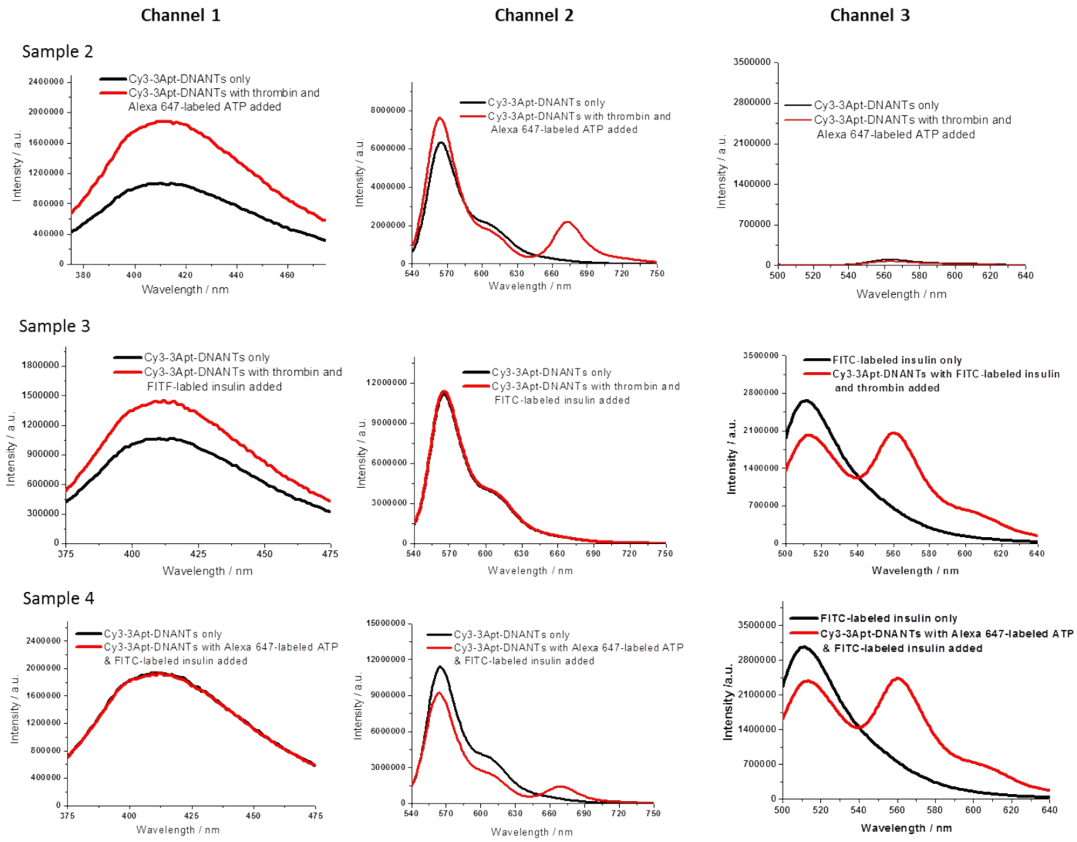

Figure S12. Simultaneous measurement of the fluorescence change of the 0.2 μM Cy-3 labeled 3Apt-DNANTs before and after an addition of the two out of three targets including 0.2 μM thrombin and 0.2 μM ATP (Sample 2) or 0.2 μM thrombin or 0.2 μM insulin (Sample 3) or, 0.2 μM ATP and 0.2 μM insulin (Sample 4). Channel 1 monitors the fluorescence intensity enhancement of 3MI by exciting at 350 nm and collecting the emission signals from 375 nm to 475 nm; channel 2 monitors the FRET signal of Alexa 647 labeled-ATP by exciting the Cy3 fluorophore at 514 nm and collecting the emission signals from 640 to 750 nm; channel 3 monitors the FRET signal of Cy3 fluorophore-labeled nanotubes by exciting the FITC fluorophore at 475 nm and collecting the emission signals from 550 to 640 nm.

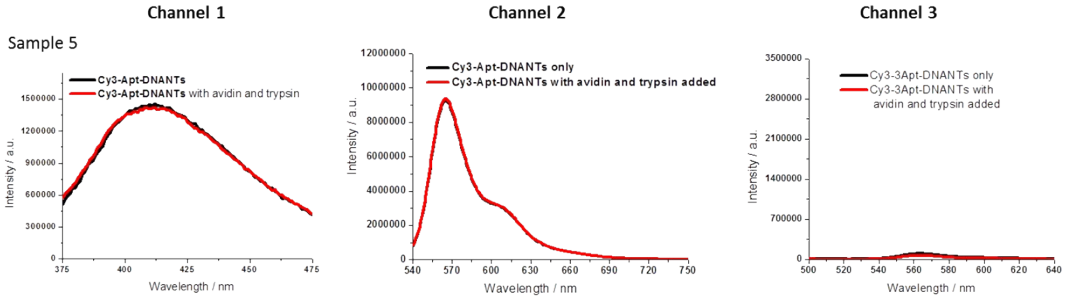

Figure S13.A measurement of the fluorescence change of the 0.2 μM Cy-3 labeled 3Apt-DNANTs before and after an addition of the control targets such as 0.2 μM avdin or 0.2 μM trysin (Sample 5). Channel 1 monitors the fluorescence intensity enhancement of 3MI by

exciting at 350 nm and collecting the emission signals from 375 nm to 475 nm; channel 2 monitors the FRET signal of Alexa 647 labeled-ATP by exciting the Cy3 fluorophore at 514 nm and collecting the emission signals from 640 to 750 nm; channel 3 monitors the FRET signal of Cy3 fluorophore-labeled nanotubes by exciting the FITC fluorophore at 475 nm and collecting the emission signals from 550 to 640 nm

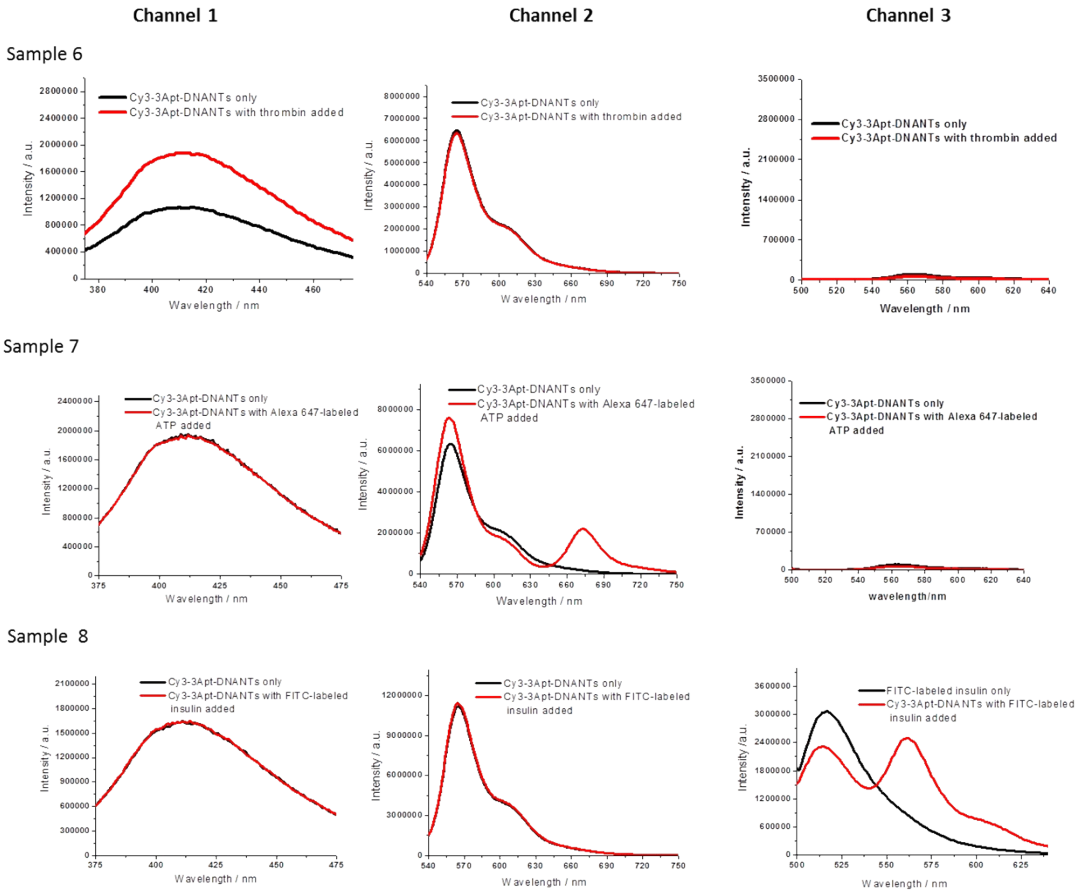

Figure S14. Single measurement of the fluorescence change of the 0.2 μM Cy-3 labeled 3Apt-DNANTs before and after an addition of the one out of three targets including 0.2μM thrombin (Sample 6)or0.2 μM ATP (Sample 7) or 0.2 μM insulin (Sample 8). Channel 1 monitors the fluorescence intensity enhancement of 3MI by exciting at 350 nm and collecting the emission signals from 375 nm to 475 nm; channel 2 monitors the FRET signal of Alexa 647 labeled-ATP by exciting the Cy3 fluorophore at 514 nm and collecting the emission signals from 640 to 750 nm; channel 3 monitors the FRET signal of Cy3 fluorophore-labeled nanotubes by excitingthe FITC fluorophore at 475 nm and collecting the emission signals from 550 to 640 nm.

Atomic force microscopy (AFM) Imaging

High-resolution AFM imaging was conducted on HOPG substrates in fluid by using a BioScope Catalyst Atomic Force Microscope system (Bruker Nano, Santa Barbara, CA) equipped with a piezo-electric AFM scanner to drive the movement of the AFM probe in Z-axis with the range of 26 µm. The maximum X-Y scan range was 150 µm × 150 µm. A silicon nitride AFM tip (SCANASYST-FLUID, Bruker Nano, SantaBarbara, CA) with a spring constant of 0.7 N/m was used and the actual value of spring constant was calibrated by a thermal tune method prior to imaging. Imaging was then performed in Tapping Mode and PeakForce Tapping Mode with the scan rate of 1 Hz. The resolution of AFM imaging was selected as 256 × 256. AFM images were processed and analyzed on AFM offline software, NanoScope Analysis (v 1.5, Bruker Nano, Santa Barbara, CA). The height images were flattened using 1st order flattening, and no further image processing was performed. Data processing were performed with GraphPadPrism(v 6, GraphPad Software, San Diego, CA). For the preparation of protein-bound nanotube complex, typically, 5.2 µM of nanotube samples (prepared according the above described procedure) were mixed with 15.6 µM of protein samples (thrombin or insulin) in 120 µL 0.1 X TAMg buffer. The solution was filtered by 0.2 µm diameter membranes and the residue on filter membrane was re-dissolved in 30 µL pre-filtered 0.1 X TAMg buffer and used for AFM imaging without further treatment.

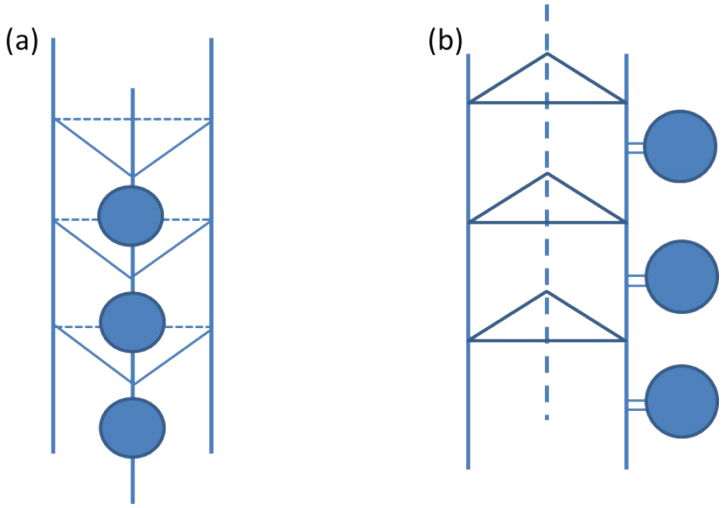

Scheme S3. Schematic representation of the alignment of the bound proteins along the aptamer-functionalized DNA nanotubes. (a) Protein bound to the top edge of the nanotube. (b) Protein bound to the side of the nanotube.

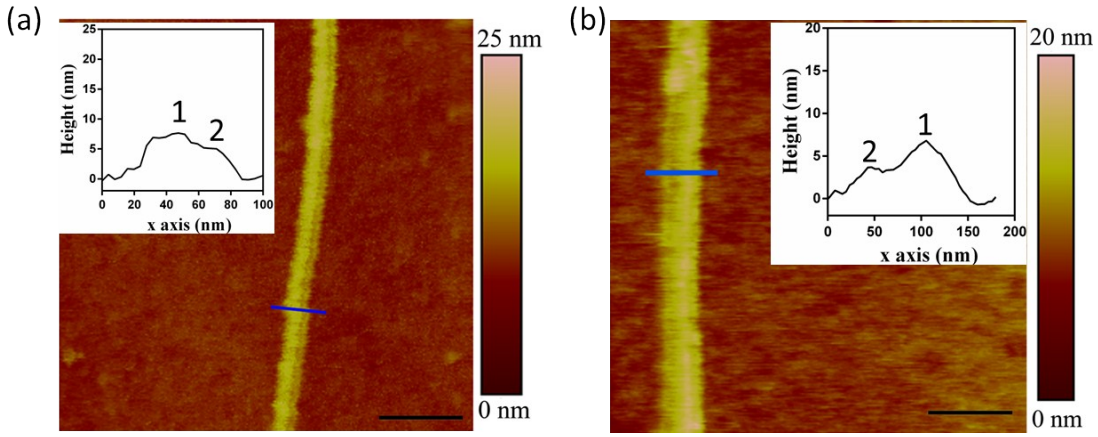

Figure S15. Liquid AFM images and the corresponding cross-section profiles of (a) thrombin and (b) insulin bound to the side of the aptamer-functionalized DNA nanotube. Scales bars: 200 nm.

References

---

[i] P. K. Lo, P. Karam, F. A. Aldaye, C. K. McLaughlin, G. Hamblin, G. Cosa, H. F. Sleiman "Loading and Selective Release of Cargo in DNA Nanotubes with Longitudinal Variation". *Nature Chemistry* **2010**, *2*, 319-328. (b) F. A. Aldaye, P. K. Lo, P. Karam, C. K. McLaughlin, G. Cosa, H. F. Sleiman "Modular Construction of DNA Nanotubes with Readily Tunable Geometry, Rigidity, and Single- or Double-Stranded Character". *Nature Nanotechnology***2009**, *4*, 349-352.